JOURNAL OF Materials CHEMISTRY

Effect of the preparation method on the properties of zirconia–ceria materials

Sylvie Rossignol, François Gérard and Daniel Duprez*

Laboratoire de Catalyse en Chimie Organique, UMR 6503, CNRS et Université de Poitiers, 40 Avenue du Recteur Pineau, 86022 Poitiers, France. E-mail: Daniel.Duprez@campus.univ-poitiers.fr

Received 20th January 1999, Accepted 12th April 1999

Zirconium–cerium mixed oxides were prepared by two methods: (i) sol–gel hydrolysis of alcoholic solutions of zirconium alkoxides (*n*-propoxide and *n*-butoxide) in the presence of aqueous solutions of cerium nitrate (method SG) or (ii) coprecipitation of aqueous solutions of zirconyl and cerium nitrates by ammonia (method NP). Dried or calcined solids were characterized by XRD, DTA, BET and oxygen storage capacity (OSC) measurements, O_2 adsorption was monitored by infrared spectroscopy. Regardless of the zirconium precursor, SG samples calcined at 900 °C have a fluorite-type structure with BET surface areas varying between 35 and 45 $m^2\ g^{-1}$. Cerium-rich samples ($0.85 \leqslant x \leqslant 0.90$), with excellent OSC properties and high thermal stability can be prepared by the sol–gel method. FTIR studies of O_2 adsorption reveal the presence of stable superoxide species whose concentration strongly depends on the cerium content and the method of preparation. A good correlation between the relative amount of O_2^- species and OSC values was observed. Superoxide ions may be formed at the same anionic vacancies as those involved in oxygen storage.

Introduction

Ceria is a crucial component of modern catalysts used for automotive emission control. A number of roles have been ascribed to ceria: promotion of the water–gas shift reaction, maintenance of noble metal dispersion and stabilization of the surface area of the alumina support. However, the main role of ceria is its ability to store oxygen (oxygen storage capacity or OSC) associated with the fast Ce^{4+}/Ce^{3+} redox process and the exceptional ability of ceria to stabilize anionic vacancies.[1–5]

Recently it was found that incorporation of up to 50% zirconia into ceria led to the formation of a solid solution of cubic structure. In these materials, the reducibility of Ce^{4+} cations is greatly enhanced and the thermal stability is improved.[6–8] However, the preparation method can affect the surface and textural properties of these $Zr_{1-x}Ce_xO_2$ oxides.

In previous work,[9] we compared two preparation methods: (i) precipitation of zirconium and cerium nitrates by aqueous ammonia and (ii) sol–gel hydrolysis of zirconium *n*-propoxide and cerium nitrate. The whole range of compositions from $x=0$ to 1 was investigated. For materials calcined at 600 °C, the best results concerning OSC properties and thermal stability were obtained for mixed oxides with x between 0.75 and 1.

The goal of this present study was to modify the preparation method to enhance both thermal stability and oxygen storage capacity. Possible implications of surface superoxide species (detected by FTIR) on oxygen mobility were also investigated. Dried or calcined solids were characterized by DTA and XRD and by their BET surface area measurements. The influence of the zirconium precursor and the purity of the cerium nitrate as well as the effect of the temperature of calcination will be discussed on the basis of OSC measurements and the FTIR spectra of samples undergoing O_2 adsorption.

Experimental

1 Preparation

Coprecipitation and sol–gel synthesis procedures were similar to those described previously.[9] Solution concentrations were adjusted so as to obtain 3 g of solid.

Sol–gel method. Two Zr precursors were used: zirconium *n*-propoxide $Zr(OC_3H_7)_4$ (70% in propan-1-ol) and *n*-butoxide $Zr(OC_4H_9)_4$ (80% in butan-1-ol). Generally, the alcohol solvent used with zirconium *n*-propoxide was isopropyl alcohol (RP, $H_2O \leqslant 0.5\%$) while butan-1-ol was employed with zirconium *n*-butoxide (RP, $H_2O \leqslant 0.5\%$). After dissolution in 20 cm^3 of alcohol, the zirconium precursor was slowly added (1 $cm^3\ min^{-1}$, ambient temperature) to an aqueous solution of $Ce(NO_3)_3 \cdot 6H_2O$ (20 cm^3, stirring speed: 500 rpm) to immediately give a pseudo-gel formed by hydrolysis of the mixture.

Different grades of cerium nitrate with lanthanum as the main impurity are available. In order to study the possible effect of La on the performance of $Zr_{1-x}Ce_xO_2$ compounds, three cerium nitrate samples of different purity were used: two crystallized cerium nitrates, of 99% ($La \approx 1\%$) and 99.99% purity, respectively, and one cerium nitrate solution provided by Rhodia (503 g L^{-1}; %Ce among the metal cations: 99.5%). When the solution was used, the volume was adjusted to 20 cm^3 in distilled water.

Coprecipitation method. Hydrated zirconia–ceria was obtained by coprecipitation, in 12 cm^3 NH_3 (aq) (14.7 M), of a mixture of $Ce(NO_3)_3 \cdot 6H_2O$ (20 cm^3 in distilled water) and $ZrO(NO_3)_2$ (20 cm^3 in distilled water). The hydrated precipitates were filtered off (porosity 4), redispersed in 100 cm^3 of NH_3 (aq) (0.25 M) and filtered again.

All other reagents and solvents were Aldrich products, 99% purity. They were used without further purification.

The synthesized materials were dried at 60 °C for 1 h in air and at 120 °C overnight in a drying oven under an air flow. The dried powders were finally calcined in air at 780 or 900 °C for 4 h.

2 Bulk characterization

Differential thermal analysis (DTA) was used to characterize the solids dried at 120 °C. DTA experiments were carried out between 25 and 500 °C using a Thermal Analyst 2100, TA Instruments. The samples were heated at 5 °C min^{-1} in dry air (Air Liquide, total impurities $\leqslant 5$ ppm). Preliminary experiments showed that no DTA peak was observed above 500 °C.

Specific surface areas were determined by N_2 (Air Liquide, 30% N_2 in He) adsorption at $-196\,^{\circ}C$ (one point BET method) with a Micromeritics Flow Sorb II.

XRD analyses of the different powders calcined at 780 and 900 °C were carried out in a Siemens D500 powder diffractometer using Cu-Kα_1 radiation ($\lambda = 0.15406$ nm). Crystalline phases were identified by comparison with ICDD files [ZrO_2: 42–1164 (tetragonal); $Zr_{0.25}Ce_{0.75}O_2$: 28–271 (cubic); CeO_2: 34–394 (cubic)].[10–12]

The diffractograms were obtained under the following conditions: dwell time: 10 s; step: 0.02°; 2θ range: 10–90°; divergence split: 1°. Diffraction peaks were fitted using Profile (a Socabim program, France) assuming split pseudo-Voigt models of the peak profile. U-Fit, a program designed by M. Evain, was used for cell parameter refinement.[13] Zero shift and sample displacement were respectively 0.0105 (2θ) and 0.015° (2θ).

Oxygen storage capacity (OSC) was measured at atmospheric pressure using alternate pulses of O_2 (Air Liquide, total impurities $\leqslant 5$ ppm) and CO (Air Liquide, N20) (0.265 cm^3) introduced onto the oxide sample (20 mg) at 400 °C to simulate lean and rich conditions in an engine. The continuous flow rate of helium was 30 cm^3 min^{-1} and the maximum concentration of O_2 or CO on the catalyst sample was about 5%. Oxygen storage can be evaluated from the CO consumption, the CO_2 formation after a CO pulse or the O_2 consumption after an O_2 pulse. Whatever the method of evaluation, alternate pulses gave very similar OSC values (μmol CO, CO_2 or O atom per gram).

Monitoring of O_2 adsorption by FTIR was carried out on a Nicolet Magna 550 spectrometer (resolution 4 cm^{-1}). Experiments were performed on a self-supporting wafer (50 mg, pressed under 1.5 tonne cm^{-2}) introduced into a home-made quartz cell equipped with KBr windows. In accordance with previous studies,[14,15] superoxide and peroxide species were expected to be formed on ceria-containing oxides. Two pretreatment procedures were used: (i) oxidation under oxygen (Air Liquide, total impurities $\leqslant 5$ ppm) (15 cm^3 min^{-1}) at 400 °C for 12 h, and outgassing at 700 °C under vacuum for 1 h or (ii) reduction under H_2 (Air Liquide, total impurities $\leqslant 1$ ppm) (30 cm^3 min^{-1}) at 400 °C for 1 h and outgassing under vacuum for 3 h. Oxygen (20 mbar) was introduced into the IR cell and spectra were recorded at room temperature within the range 4000–800 cm^{-1}. Results were analysed by using the Omnic program.[16]

A classification of the samples with the precursor used for the preparation is given in Table 1.

Results

1 $Zr_{1-x}Ce_xO_2$ mixed oxides prepared by coprecipitation or sol–gel methods

Fig. 1(a) and (b) show the DTA profiles obtained for series 1 and 2 (Table 1). The thermograms corresponding to SG materials show a strong endothermic peak at about 240 °C attributed to the formation of a $Zr_{1-x}Ce_xO_2$ solid solution with a cubic structure.[6] In the case of coprecipitated solids, small exothermic peaks between 200 and 250 °C may be ascribed to the decomposition of residual nitrates.

Table 1 Samples prepared by the sol–gel method [Zr propoxide (Pr) or Zr butoxide (Bu)] or by coprecipitation [zirconyl nitrate (NP) (nitrate precipitation)]

	Precursors		
%mol Ce	Series 1 $Ce(NO_3)_3 \cdot 6H_2O$ $Zr(OC_3H_7)_4$	Series 2 $Ce(NO_3)_3 \cdot 6H_2O$ $Zr(OC_4H_9)_4$	Series 3 $Ce(NO_3)_3 \cdot 6H_2O$ $ZrO(NO_3)_2$
75	ZrCe75Pr	ZrCe75Bu	ZrCe75NP
85	ZrCe85Pr	—	ZrCe85NP
90	ZrCe90Pr	ZrCe90Bu	ZrCe90NP
95	ZrCe95Pr	—	ZrCe95NP
100	—	—	ZrCe100NP

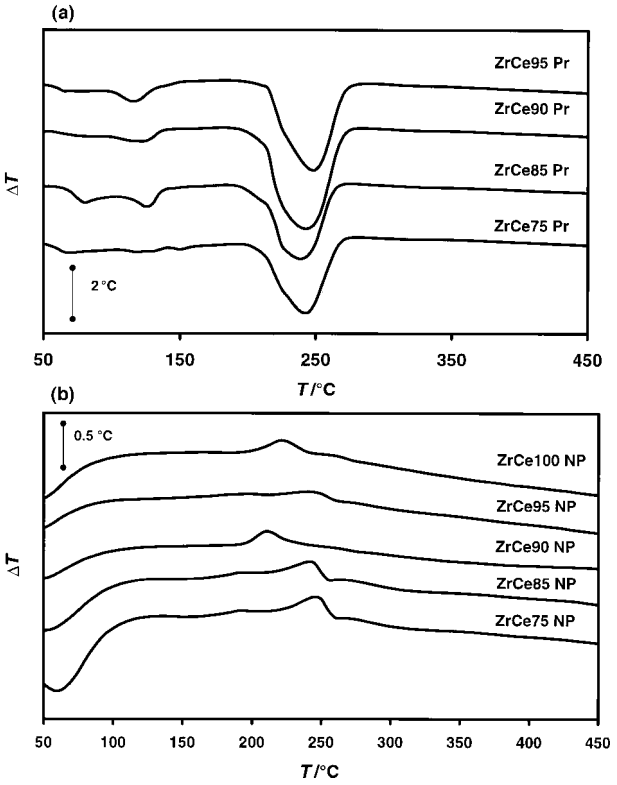

Fig. 1 DTA profiles of $Zr_{1-x}Ce_xO_2$ oxides prepared by (a) the sol–gel method and (b) coprecipitation, for $0.75 \leqslant x \leqslant 1$.

XRD patterns for the solids calcined at 900 °C are presented in Fig. 2(a) and (b). All solids apparently exhibit a cubic structure. However, closer observation at $2\theta \approx 29°$ reveals the presence of a mixture of tetragonal ZrO_2 and cubic CeO_2 phases for the solids prepared by coprecipitation (Fig. 3). Similar results were obtained with solids calcined at 600 °C.[9] These results show that solid solutions can be obtained *via* sol–gel synthesis at mild temperatures while coprecipitation leads to a mixture of phases independent of calcination temperature (below 900 °C). The cell parameters of the fluorite-type cubic structure were determined for the samples of series 1 which are true solid solutions (Fig. 4). Literature data for pure ceria and $Zr_{0.25}Ce_{0.75}O_2$ solid solutions[11,12] are also presented in this figure. The cell parameter increases linearly with the cerium content, according to Vegard's law applied to fluorite-type structures. Nevertheless, the experimental parameters are larger than those reported in the literature for $Zr_{1-x}Ce_xO_2$ solid solutions.[16–18] This difference may be due to the method of preparation and to the calcination temperature.

Fig. 5 shows the variation of the specific surface area as a function of x_{Ce} for series 1 and 2. For coprecipitated solids, the BET area slowly decreases as x_{Ce} increases between 0.75 and 1. Sol–gel samples are significantly more stable whatever the calcination temperature, the highest BET values being obtained for x_{Ce} between 0.9 and 0.95. The sol–gel method allows the preparation of very stable $Zr_{1-x}Ce_xO_2$ solid solutions with high cerium contents, which seems difficult to achieve by coprecipitation.

2 Oxygen storage capacity

Fig. 6(a) shows the changes in OSC [$cm^3(O_2)g^{-1}$] with x_{Ce} for the three series of samples calcined at 780 and 900 °C. In

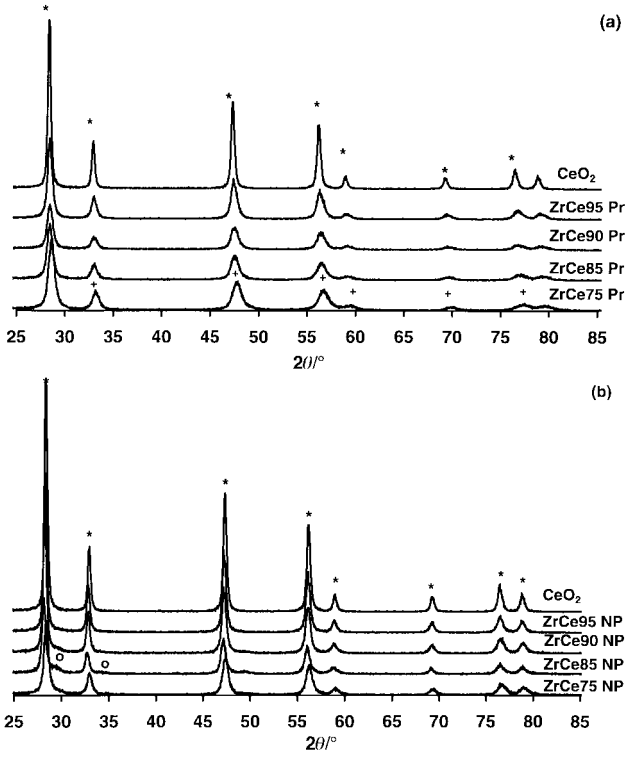

Fig. 2 XRD patterns of $Zr_{1-x}Ce_xO_2$ oxides prepared by (a) the sol–gel method and (b) coprecipitation, for $0.75 \leqslant x \leqslant 1$. ICDD files: (+) $Zr_{0.25}Ce_{0.75}O_2$ [28–271]; (*) CeO_2 [34–394]; (○) ZrO_2 [42–1164].

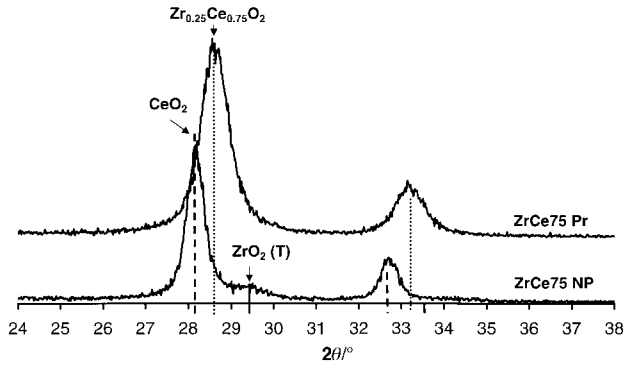

Fig. 3 Enlargement of the XRD spectra between 24 and 38° for the ZrCe75 samples.

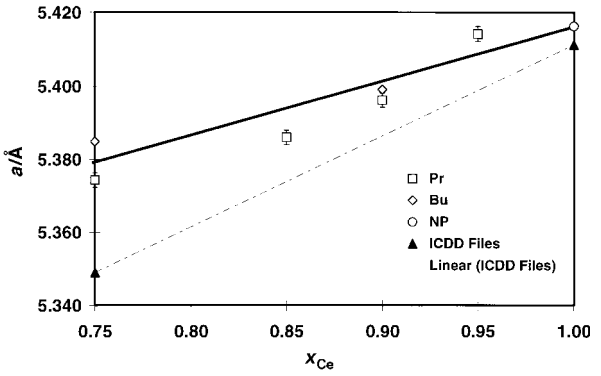

Fig. 4 Cell parameter (determined using U-fit peak refinement program) as a function of the cerium atomic fraction.

comparison with materials obtained by coprecipitation, sol–gel samples present a very high oxygen mobility, especially at high cerium content. Only small differences can be observed between the two zirconium precursors. After calcination at 900 °C, a

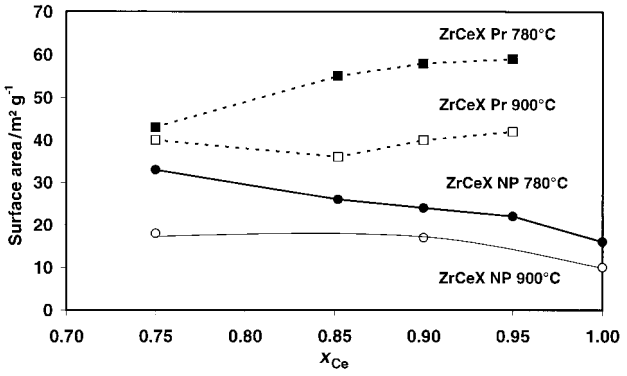

Fig. 5 Surface areas of $Zr_{1-x}Ce_xO_2$ oxides (series 1 and 2) calcined at 900 and at 780 °C.

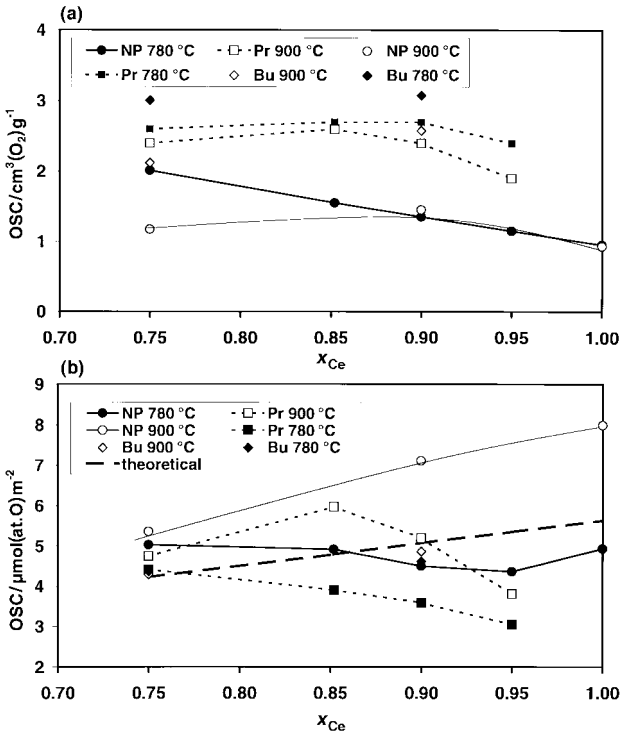

Fig. 6 OSC (400 °C) of $Zr_{1-x}Ce_xO_2$ oxides calcined at 780 and 900 °C: (a) specific values in cm^3 (STP) of O_2 g^{-1}; and (b) intrinsic alues in μmol(at. O)m^{-2}.

maximum capacity of 2.5 cm^3 g^{-1} can be reached for samples with $0.85 \leqslant x \leqslant 0.90$.

OSC values are not directly correlated with BET area: for all samples, OSC is less affected by high-temperature treatments than the specific surface area. Therefore, OSC values expressed in μmol(at.O) m^{-2} are higher after calcination at 900 than at 780 °C [Fig. 6(b)]. This explains the high intrinsic values measured for coprecipitated samples which have a low BET surface area when calcined at 900 °C. For sol–gel materials, very similar results were obtained with Zr propoxide and Zr butoxide. After calcination at 780 °C, a slight decrease of OSC with x_{Ce} can be observed while, at 900 °C, a maximum is obtained for $x_{Ce}=0.85$. The high OSC values are certainly related to the cubic structure of these solids in which the oxygen mobility has been shown to be enhanced.[8,9] Here, the question arises as to whether oxygen storage is a process strictly confined to the surface or if it involves bulk oxygens. Taha *et al.*[19] calculated the theoretical OSC of ceria on the basis of one surface oxygen out of four reacting, corresponding to the reduction of Ce^{4+} to Ce^{3+}. For a cubic crystal of ceria with an interplanar distance of 0.541 nm, they found an OSC value of 5.64 μmol(at.O) m^{-2}. Assuming that there is no

surface enrichment in Ce or Zr, the theoretical OSC of a $Zr_{1-x}Ce_xO_2$ solid solution would be $5.64x$ μmol(at.O) m^{-2}. The line corresponding to this equation is drawn in Fig. 6(b) (theoretical). Experimental points above this line indicate a reduction of subsurface atoms while points below the line are obtained for samples storing oxygen exclusively at the surface. Although the experimental data are generally not very far from the theoretical line, two conclusions can be drawn from Fig. 6(b): (i) for samples with the highest BET area (smallest crystallite size), the reduction is limited to surface Ce atoms. This is the case for sol–gel samples calcined at 780 °C. Increasing the temperature of calcination or changing the mode of preparation leads to a deeper reduction, in the bulk of $Zr_{1-x}Ce_xO_2$. (ii) The above conclusion particularly holds for cerium-rich samples: decreasing x_{Ce} tends to attenuate the differences and for $x_{Ce}=0.75$, all the samples have very similar OSC properties.

3 Study of the sol–gel preparation for $x_{Ce}=0.90$

The sol–gel method is an effective way for preparing stable cerium-rich $Zr_{1-x}Ce_xO_2$ solid solutions (Fig. 5). Therefore, a detailed study was carried out for ZrCe90 compounds. The mode of preparation was modified by varying the nature of the zirconium precursor and the purity of the cerium nitrate. Possible effects of the solvent (isopropyl alcohol or butanol) and of the oxidation state of Ce in the cerium precursor (Ce^{4+} or Ce^{3+}) were also investigated.

BET surface area and OSC values for the different samples are reported in Table 2. The presence of 1% La in the cerium nitrate slightly increases the oxide stability (compare samples 1,2 and 5,6) but significantly decreases the OSC of catalysts calcined at 780 °C. The effect is more limited for catalysts calcined at 900 °C. Lanthanum seems to hinder the complete reduction of surface cerium ions: OSCs of lanthanum-containing oxides are systematically lower than 5.07 μmol(at.O) m^{-2}, the theoretical value corresponding to a complete reduction of the ZrCe90 surface. In fact, mixed oxides prepared with high purity cerium nitrate show OSCs equal to or higher than this theoretical value.

These materials were prepared from cerium(III) nitrate. The preparation was carried out in air so that most of the Ce^{3+} ions were probably oxidized to Ce^{4+}. In order to be certain that all the Ce^{3+} ions were transformed into Ce^{4+}, 5 cm^3 H_2O_2 (110 volumes of O_2) was added to the cerium(III) nitrate solution to ensure complete oxidation. The resulting solid (sample 10 in Table 2) does not show any unusual behavior and has very similar properties compared to sample 6, prepared without adding hydrogen peroxide. This indicates that the rate of Ce^{3+} oxidation is not a limiting factor in preparing $Zr_{1-x}Ce_xO_2$ solid solutions from cerium(III)nitrate.

The possible effect of the length of the hydrocarbon chain in the alkoxide was investigated by substituting Zr butoxide for Zr propoxide. BET areas were unchanged (compare samples 5,6 and samples 7,8) but it appears that the use of Zr butoxide could improve OSC properties. The effect is more pronounced after calcination at 780 than at 900 °C. Changing solvent (samples 2,3 or 7,9) has practically no effect on the OSC properties.

Table 3 Crystallite size and calculated surface area of some $Zr_{0.1}Ce_{0.9}O_2$ compounds

Sample	Crystallite size			Surface area/ m^2/g^{-1}
	2θ/°	*hkl* planes	*d*/nm	
5 (propoxide, 780 °C)	28.66	111	23.6	3.59
	47.66	200	17.5	48.6
	56.54	311	18.1	46.8
6 (propoxide, 900 °C)	28.69	111	26.9	31.5
	47.65	200	22.5	37.7
	56.53	311	19.9	40.9
8 (butoxide, 900 °C)	28.66	111	27.9	30.5
	47.66	200	22.5	37.8
	56.55	311	23.3	36.4

The average crystallite size, determined by XRD along three *hkl* directions (Table 3), is 19 nm for sample 5 calcined at 780 °C and 23–25 nm for samples 6 and 8 both calcined at 900 °C. The surface area A of these samples can be calculated using eqn. (1), assuming a spherical particle:

$$A(\mathrm{m^2\ g^{-1}})=\frac{6}{\rho d} \quad (1)$$

where $\rho=7.07\times10^6$ g m^{-3}, the density of ZrCe90, and d is the particle diameter in meters. There is a reasonable agreement between the values of A calculated by XRD and those determined by the BET method (Table 2). This observation shows that these oxides do not develop any microporosity. XRD data confirm the excellent thermal stability of ZrCe90 samples prepared by the sol–gel method.

4 Infrared study of O_2 adsorption

Oxygen adsorption at room temperature on samples calcined at 900 °C was monitored by FTIR. Fig. 7(a) represents the baseline spectrum corresponding to ZrCe75Bu pretreated at 700 °C. It shows a clean surface with very weak ν(OH) bands (mainly bidentate OH species at 3650 cm^{-1}), negligible formate bands (at 2945 cm^{-1}) and practically no carbonate bands (1200–1600 cm^{-1}). Carbonate bands are usually abundant on ceria-containing oxides before pretreatment at high temperature. The spectrum in Fig. 7(b) was recorded 60 s after O_2 admission (20 mbar). Subtracting spectrum (a) from spectrum (b) clearly shows the changes due to O_2 adsorption (spectrum b − a). A small increase of the ν(OH) band intensity is observed and the two sharp bands at 1126 and 2232 cm^{-1} can be

Table 2 Effect of the method of preparation (sol–gel) on the performances of $Zr_{0.1}Ce_{0.9}O_2$ compounds (Pr = Zr propoxide, Bu = Zr butoxide, IPA = isopropyl alcohol, BA = *n*-butanol)

Sample no.	Ce nitrate purity (%)	Zr precursor/ alcohol	*T*/°C calcination	BET area/ m^2/g^{-1}	OSC/ cm^3/g^{-1}	OSC/ μmol(at.O) m^{-2}
1	99.99	Pr/IPA	780	56	3.42	5.09
2	99.99	Pr/IPA	900	35	2.53	5.97
3	99.99	Pr/BA	900	36	2.51	5.76
4	99.5	Pr/IPA	900	39	2.45	5.18
5	99	Pr/IPA	780	58	2.55	3.64
6	99	Pr/IPA	900	44	2.50	4.70
7	99	Bu/IPA	780	55	3.08	4.62
8	99	Bu/IPA	900	44	2.58	4.84
9	99	Bu/BA	780	61	2.97	4.02
10	99	Pr/IPA $+H_2O_2$	900	42	2.48	4.88

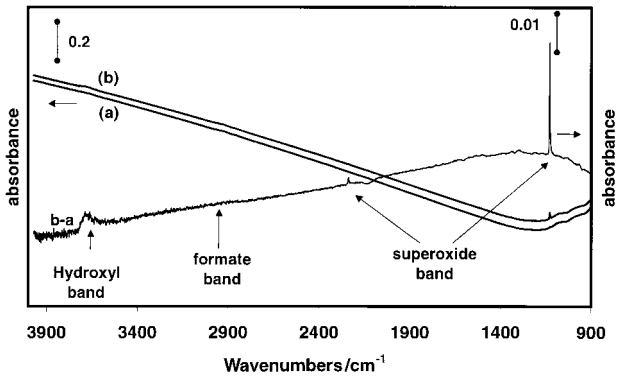

Fig. 7 FTIR spectra of the ZrCe75Bu sample (a) before and (b) after oxygen adsorption (20 mbar) at room temperature. Spectrum (b−a) reveals the new IR features which appear upon O_2 adsorption.

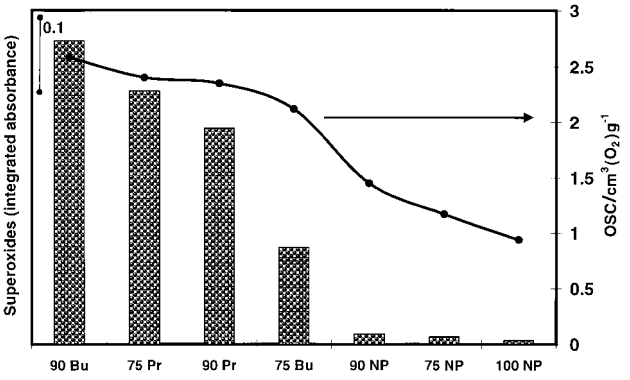

Fig. 9 Correlation between the OSC values and the amount of superoxide (integrated absorbance of the band at 1126 cm^{-1}).

ascribed to superoxide, which is in agreement with the results of Li *et al.*[20] The main band at 1126 cm^{-1} corresponds to superoxide ions with an oxygen–oxygen bond order of 1.5. The second band at 2232 cm^{-1} can be ascribed to the first overtone of the main band at 1126 cm^{-1}, which is in agreement with the results of other authors.[14] Two types of oxygen species can be observed by FTIR upon oxygen adsorption on ceria: O_2^- (superoxide) and O_2^{2-} (peroxide).[14,21] Peroxide bands (main bands at 880 cm^{-1}) can be observed on pre-reduced ceria but are generally not or only weakly visible on oxidized samples.[22] Fig. 8 presents FTIR spectra of the ZrCe75Bu sample as a function of the adsorption time, ranging from 60 to 1200 s. Superoxide species remain very stable under 20 mbar of O_2.

This study was extended to all the $Zr_{1-x}Ce_xO_2$ samples. The integrated absorbance of the peak at 1126 cm^{-1} normalized with respect to the wafer weight (50 mg) gives an idea of the relative amount of superoxide ions generated at the oxide surface. For all the materials, the amount of superoxide remains essentially constant for over 20 min, with only a very small decrease of the superoxide concentration being observed, which is in agreement with the results of Li *et al.*[14] Integrated absorbance values taken after 600 s are reported in Fig. 9 for various samples. Large differences between materials are revealed, based on their ability to form superoxide species: the integrated absorbance varies from 0.45 for ZrCe90Bu to 0.005 for ZrCe100NP. The difference in O_2^- concentration depends both on the Zr content and on the method of preparation. $Zr_{1-x}Ce_xO_2$ samples yield a larger amount of superoxide species than does pure ceria. For a given composition in Ce, sol–gel materials are significantly more active for O_2^- formation than coprecipitated solids. These results suggest that there is a correlation between the ability for an oxide to form superoxide species and its oxygen storage capacity, a hypothesis which is verified by Fig. 9. OSC measurements can be linked to the ability of the solid to form anionic vacancies, O_2 filling the vacancies created by the oxidation of CO [eqn. (2) and (3)]:

$$\delta CO + Zr_{1-x}Ce_xO_2 \rightarrow Zr_{1-x}Ce_xO_{2-\delta} + \delta CO_2 \quad (2)$$

$$Zr_{1-x}Ce_xO_{2-\delta} + \frac{\delta}{2}O_2 \rightarrow Zr_{1-x}Ce_xO_2 \quad (3)$$

The reduction of Ce^{4+} to Ce^{3+} can compensate for the negative charge due to formation of anionic vacancies. However, some of these anionic vacancies remain negatively charged. They behave as electron donating species and represent potential sites for O_2 adsorption to form superoxide species. The fraction δ of vacancies created by reaction with CO at 400 °C is certainly much higher than the fraction δ' present after outgassing at 700 °C. Nevertheless, there is probably a parallel evolution of the number of anionic vacancies under reducing and vacuum conditions so that a definite relationship between OSC and superoxide amounts can logically be found.

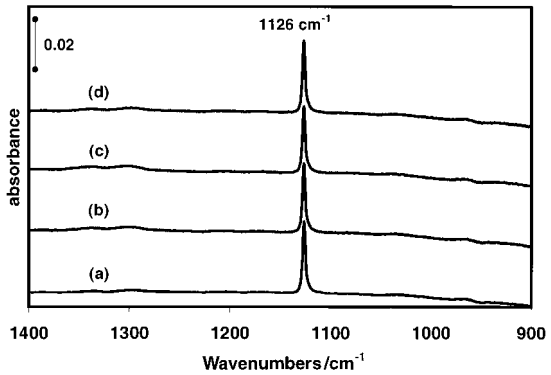

Fig. 8 O_2 adsorption (20 mbar) on ZrCe75Bu. Effect of time on FTIR spectra: (a) 60 s, (b) 300 s, (c) 600 s and (d) 1200 s.

Conclusion

$Zr_{1-x}Ce_xO_2$ mixed oxides with $x > 0.5$ present a fluorite-type structure of very high thermal resistance. Two modes of preparation were investigated, namely: (i) the sol–gel method based on slow hydrolysis of alcoholic solutions of zirconium alkoxides by aqueous solutions of cerium nitrate (series SG) and (ii) coprecipitation of aqueous solutions of zirconyl and cerium nitrates by ammonia (series NP).

The mode of preparation has a strong effect on structure, texture and surface properties of the mixed oxides. The SG method gives homogeneous compounds of fluorite-type structure (even for x close to 0.9, which is difficult to reach by other methods) while NP leads to solids in which tetragonal zirconia is always present.

Changing alcohol (isopropyl alcohol or *n*-butanol) or alkoxide precursor (propoxide or butoxide) has only a slight effect on the thermal stability and the OSC properties of SG binary oxides. It was also shown that the oxidation state of cerium (Ce^{3+} or Ce^{4+}) in the nitrate precursor has no influence on the properties of the resulting materials. Nevertheless the presence of small amounts of lanthanum in cerium nitrate ($\approx$1% La) improves the thermal stability but decreases the oxygen storage capacity of the binary oxides.

FTIR experiments show that stable superoxide species are formed upon O_2 adsorption at room temperature. Their amounts can be correlated with oxygen mobility: the highest oxygen mobility is obtained for ZrCe90Bu where the greatest amount of superoxide has been detected.

Acknowledgement

Thanks are due to S. Cremer for his technical help in carrying out most of the experiments which are reported in this paper.

References

1 F. Zamar, A. Trovarelli, C. Leitenburg and G. Dolcetti, *Stud. Surf. Sci. Catal.*, 1996, **101**, 1283.
2 T. Bunluesin, R. J. Gorte and G. W. Graham, *Appl. Catal.*, *B*, 1997, **14**, 105.
3 Y. Sun and P. A. Sermon, *J. Mater. Chem.*, 1996, **6**, 1025.
4 A. Trovarelli, F. Zamar, J. Llorca, C. Leitenburg, G. Dolcetti and J. T. Kiss, *J. Catal.*, 1997, **169**, 49.
5 P. Fornasiero, G. Balducci, J. Kaspar, S. Meriani, R. Di Monte and M. Graziani, *Catal. Today*, 1996, **29**, 47.
6 G. Balducci, J. Kaspar, P. Fornasiero, M. Graziani and M. Saiful Islam, *J. Phys. Chem. B*, 1998, **102**, 557.
7 L. Mubmann, D. Lindner, E. S. Lox, R. Van Yperen, T. P. Kreuser, I. Mitsushima, S. Taniguchi and G. Garr, SAE Technical Paper 970465, 1997.
8 C. Leitenburg, A. Trovarelli, F. Zamar, S. Maschio, G. Dolcetti and J. Llorca, *J. Chem. Soc.*, *Chem. Commun.*, 1995, 2181.
9 S. Rossignol, Y. Madier and D. Duprez, *Catal. Today*, 1999, **50**, 261.
10 G. Teufel, *Acta Crystallogr.*, 1962, **15**, 1187.
11 Smith and McCarthy, ICDD file 28–271, Penn State University, ICCD Grant-in Aid, 1975.
12 *Natl. Bur. Stand. Monogr. 25* (*U.S.*), 1983, **20**, 38.
13 M. Evain, IMN Nantes, France, 1992.
14 A. Badri, C. Binet and J. C. Lavalley, *J. Chem. Soc.*, *Faraday Trans.*, 1997, **93**, 1159.
15 C. Li, Y. Sakata, T. Arai, K. Domen, K. Maruya and T. Onishi, *J. Am. Chem. Soc.*, 1989, **111**, 7683.
16 Omnic program, Nicolet Anal Instr. Techn. Publ. Dept., 1993.
17 S. Meriani and G. Spinolo, *Powder Diffr.*, 1987, **2**, 255.
18 A. Kawabata, S. Hirano, M. Yoshinaka, K. Hirota and O. Yamaguchi, *J. Mater. Sci.*, 1996, **31**, 4945.
19 R. Taha, D. Duprez, N. Mouaddib-Moral and C. Gauthier, *Stud. Surf. Sci. Catal.*, 1998, **116**, 549.
20 C. Li, Y. Sakata, T. Arai, K. Domen, K. Maruya and T. Onishi, *J. Chem. Soc.*, *Faraday Trans. 1*, 1989, **85**, 929.
21 C. Li, K. Domen, K. Maruya and T. Onishi, *J. Catal.*, 1990, **123**, 436.
22 S. Rossignol and D. Duprez, unpublished results.

Paper 9/00536F